

---

doi: 10.15407/ujpe62.12.1057

I.U. TADJIBAEV, S.N. NURITDINOV, A.A. MUMINOV

National University of Uzbekistan

(2, Universitetskaya Str., Tashkent, Uzbekistan; e-mail: [tadj\\_ikram@mail.ru](mailto:tadj_ikram@mail.ru), [nur200848@mail.ru](mailto:nur200848@mail.ru), [maa201609@gmail.com](mailto:maa201609@gmail.com))

## NONLINEAR COSMOLOGY OF GLOBULAR CLUSTER SYSTEMS AROUND GALAXIES

---

PACS 98.65.Cw

*The formation of systems of globular star clusters around galaxies has been studied in the framework of a nonlinear-nonstationary model of collapsing galaxies. Instabilities of the model with respect to four perturbation modes are analyzed, with the mode order determining the average number of clusters in the system. Critical diagrams for the dependence of the initial value of the virial ratio on the rotation degree of collapsing model are plotted. The instability growth rates are calculated, and the obtained instability parameters are compared.*

*Keywords:* systems of globular star clusters, gravitational instabilities, pulsation model of self-gravitating system, cosmology of globular clusters.

### 1. Introduction

Globular star clusters (GSCs) are rather complicated star systems that are observed around galaxies of the Hubble type. They differ from other star clusters by a significantly larger number of stars, a symmetric shape that is close to the spherical one, and a high concentration of physically coupled stars. A system of globular star clusters (SGSC) is defined as a galaxy subsystem. Sometimes, in the case of spiral galaxies, these systems may probably consist of physically weakly coupled GSCs.

According to the data of modern observations, almost all types of galaxies in the Hubble tuning fork contain SGSCs, with the number of star clusters undoubtedly depending on the galaxy type. From this point of view, SGSCs in other galaxies were studied more actively than such a system in our Galaxy. In particular, the advent of CCD cameras stimulated a drastic growth of attention to SGSCs (see, e.g., works [1–7] and the references therein). The work by Harris *et al.* [3], which was devoted to a careful data collection, should be distinguished separately. In work

[5], we analyzed the observation data and proposed a classification for the SGSCs, and in work [6] we reported results obtained while studying the SGSCs of spiral and dwarf galaxies.

The analysis of observation data for SGSCs gives us ground to understand not only specific statistical properties of GSCs, but also the physics of galaxy evolution and its stages. In this case, the chemical composition and the dynamic characteristics of the SGSCs were found to play a significant role at early stages of galaxy formation. Furthermore, the results obtained from the analysis of the SGSC observations can be used, in particular, to verify hypotheses concerning the origin of the SGSC parent galaxies.

Issues associated with the SGSC origin are directly connected with the cosmological problem of galaxy formation. There are two relevant scenarios: a cascade fragmentation [8] and a hierarchical clustering [9]. According to the former [8], galaxies are formed first at the early stage of Universe's evolution. Then, owing to their instability, those protosuperclusters are fragmented stage-by-stage down to protogalaxies. Only afterward, the SGSCs emerge. The theory of hierarchical clustering [9] asserts that it is GSC protoclouds that arise first in the Universe. Then those

protoclusters gradually unite into protogalaxies, protogalaxies into galaxy clusters, and the latter into superclusters. Therefore, it is evident that the results of researches concerning the SGSCs are required, in particular, when comparing the scenarios of galaxy formation and evolution.

## **2. Current State-of-the-Art of the Theory of the SGSC Origin**

Till now, the origin of not only SGSCs but even GSCs themselves has not been studied at length. The problems of GSC and SGSC formation have been researched in a strongly disjointed and, most often, speculative manner. Here, the number of questions strongly exceeds the number of available answers. For instance, it is unclear whether a GSC contains stars of the same generation, or it consists of stars existing at different evolution stages and with a large difference between their ages. Why do almost all GSCs have an approximately spherical shape? How is this fact associated with the efficiency of the star formation? And so forth. That is why there are a few different viewpoints in the literature concerning the formation of GSCs and their systems.

For example, a theory of GSC formation as a result of the protogalaxy collapse is discussed in work [1]. Three models of this process are distinguished. According to the first model, GSCs are formed much earlier than the galaxy itself. In the second model, the GSCs and the galaxy are formed almost simultaneously. Finally, GSCs can be formed well after the formation of their parent galaxies. A possibility of the cluster destruction as a result of, e.g., the dynamic friction, internal relaxation, tidal interaction, and star formation was also considered.

In work [10], it was supposed that some GSCs can be formed in the course of the galaxy interaction or merging, and the existence of young GSCs in the Magellanic Clouds, as well as anomalously rich SGSCs around some galaxies and especially at the centers of galaxy clusters, was explained. The authors of work [11] proposed a theory to describe the formation of globular clusters and their systems in the course of a protogalaxy collapse. In this case, the thermal instability favors the development of a two-phase structure in the gas, if the cooling and free-fall times are comparable. In accordance with the scenario considered in work [11], the hot gas component

with a temperature close to the virial one compresses the cold component into discrete clouds with temperatures of about  $10^4$  K and average densities in an interval of  $1\div 10 M_{\odot}/\text{pc}^3$ .

The authors of work [12] analyzed the multimodal distributions of the GSC metallicity in massive huge galaxies and studied the origin of various GSC subpopulations. They found that if the metal-rich and metal-poor subsystems are distinguished, the average metallicity for metal-rich GSCs in galaxies with the bimodal distribution of the GSC metallicity correlates well with the parent galaxy luminosity. On the other hand, no correlation is observed for the metal-poor GSCs. This fact testifies that metal-rich clusters are rather closely connected with the galaxy. However, the ratio between the metal-rich and metal-poor clusters correlates with the specific frequency parameter. Galaxies with a high specific frequency of GSCs contain a larger number of metal-poor clusters. The authors of work [12] assert that the model describing the merging of two galaxies cannot explain the origin of GSCs in huge galaxies. They assume that GSCs are formed during two different phases of the star formation from a gas with different metallicities, which results in a bimodal distribution. Metal-poor GSCs are formed during the early stage of the protogalactic cloud collapse, and metal-rich ones are formed later from the enriched gas and approximately simultaneously with the galaxy. Metal-rich GSCs in elliptical galaxies are considered to be similar to metal-poor ones in the halo of spiral galaxies. At the same time, GSCs, if any, in the “disks” of spiral galaxies are formed much later.

In work [13], the final stages of a collapse were studied, and the results obtained were compared with the results of the  $N$ -body problem. A possibility of the SGSC formation, when two galaxies merge, was discussed in a number of works [10, 12, 14–17]. Unfortunately, the cited authors did not consider real observation data.

The analysis of the works cited above brings us to the conclusion that, nowadays, there is no consistent theory describing the formation of GSCs. There is no comprehensive theory of the SGSC origin, where the development of exact non-stationary models has a large importance. The matter is that, irrespective of the type of the scenario describing the origin of galaxies – whether this is the cascade fragmentation or the hierarchical clustering, – it is clear

that protoclouds of globular star clusters are created owing to the gravitational instability of radial orbits against the background of either a collapsing protogalaxy or an expanding spherical cosmological model. The processes of gravitational instability run against the background of the early, nonlinear nonstationary stage of the dynamic evolution of gravitating systems. In works [6, 18], we illustrated some results obtained at studying the gravitational instability within the pulsation model. For this purpose, we used, for the first time, the analogy between a gravitating system and a gas model with an adiabatic index of  $5/3$ . Really, many authors (see, e.g., work [19] and the references therein) used an analogy with the model of a gas with the indicated adiabatic index to analyze the evolution of star systems. Therefore, the inverse approach should also make sense. Namely, we may try to apply the theoretical results obtained for a collisionless spherical system to a spherical gas system [6, 18].

### 3. Nonlinear Nonstationary Parent Model and Master Equations

In order to construct a nonlinear nonstationary model, an equilibrium configuration that is stable in the linear approximation is required as a basis. A method to construct nonlinear pulsation models for nonstationary collisionless self-gravitating systems, in which the method of Lagrange coordinates is used, was proposed in works [20–22]. The essence of this method was described in monograph [22] in detail. The stationary spherical equilibrium model developed by Camm [23] was generalized in work [24] to the case of nonlinear pulsations. In work [25], the rotating nonstationary phase model was given:

$$\Psi(r, v_r, v_\perp, t, \lambda) = \frac{\rho(t)\Pi^2}{\pi^2} \frac{\chi(f)}{\sqrt{f}} \times [1 + \Omega r v_\perp \sin \theta \sin \eta], \quad (1)$$

where

$$f = \left(1 - \frac{r^2}{\Pi^2}\right) \left(\frac{1}{\Pi^2} - v_\perp^2\right) - \left(v_r + \frac{\lambda r \sin \psi}{\sqrt{1 - \lambda^2 \Pi^2}}\right)^2, \quad (2)$$

$\chi(f)$  is the Heaviside function, the system radius changes according to the law  $R = \Pi(t) R_0$ , where the function

$$\Pi(\psi) = (1 + \lambda \cos \psi)/(1 - \lambda^2)$$

has a sense of the sphere stretching coefficient,  $\psi = e \int_0^t \Pi^{-1} dt$  is an auxiliary variable instead of the time  $t$ ,  $\lambda = 1 - \left(\frac{2T}{|U|}\right)_0$  is the pulsation amplitude ( $0 \leq \lambda \leq 1$ ),  $\left(\frac{2T}{|U|}\right)_0$  is the virial ratio at the time moment  $t = 0$ ,  $\Omega$  the parameter of solid-state rotation of a pulsating sphere ( $0 \leq \Omega \leq 1$ ),  $v_a = -\lambda r \sin \psi / (\epsilon \Pi^2)$ , and  $v_b = r/\Pi^2$  (see the other notations in works [22, 25]).

To study instabilities of the nonstationary model (1), we impose a small and, in the general case, asymmetric perturbation  $\delta\Phi$  on it. By linearizing the equation of motion

$$\ddot{\mathbf{r}} = -\frac{\mathbf{r}}{\Pi^3} + \text{grad}(\delta\Phi), \quad (3)$$

we obtain an equation for small asymmetric vibrations of a separate particle,

$$(1 + \lambda \cos \psi) \frac{d^2 \delta \mathbf{r}}{d\psi^2} + \lambda \sin \psi \frac{d\delta \mathbf{r}}{d\psi} + \delta \mathbf{r} = \frac{1}{(1 - \lambda^2)^3} (1 + \lambda \cos \psi) \frac{\partial(\delta\Phi)}{\partial \mathbf{r}}. \quad (4)$$

Now, in order to calculate of the density perturbation, we shift the centroid by  $(\bar{\delta x}, \bar{\delta y}, \bar{\delta z})$  and average Eq. (4) over the velocity space. The solution of Eq. (4) can be written in the following form, by using an analog of Green's function  $S(\psi, \psi_1)$ :

$$\bar{\delta \mathbf{r}} = \frac{1}{(1 - \lambda^2)^3} \int_{-\infty}^{\psi} (1 + \lambda \cos \psi_1)^3 \times S(\psi, \psi_1) \left[ \frac{\partial(\delta\Phi)}{\partial \mathbf{r}} \right] d\psi_1. \quad (5)$$

The potential perturbation is taken in the form

$$\delta\Phi = A(\psi) r^N \exp(im\phi) P_N^m(\cos \theta), \quad (6)$$

where  $A(\psi)$  is the sought function,  $N$  the principal perturbation index,  $m$  the azimuthal wave number, and  $P_N^m(x)$  the associated Legendre polynomial. By substituting Eq. (6) into Eq. (5) and comparing the calculated expression for the perturbation density with the theoretical one [26], we find the following nonstationary analog of the dispersion equation (NADE):

$$\frac{1}{6} A(\psi) \Pi^3 = \frac{1}{N(N+1)} S_{1N} + \frac{im\Omega(N-2)!}{(N+2)!} S_{2N}, \quad (7)$$

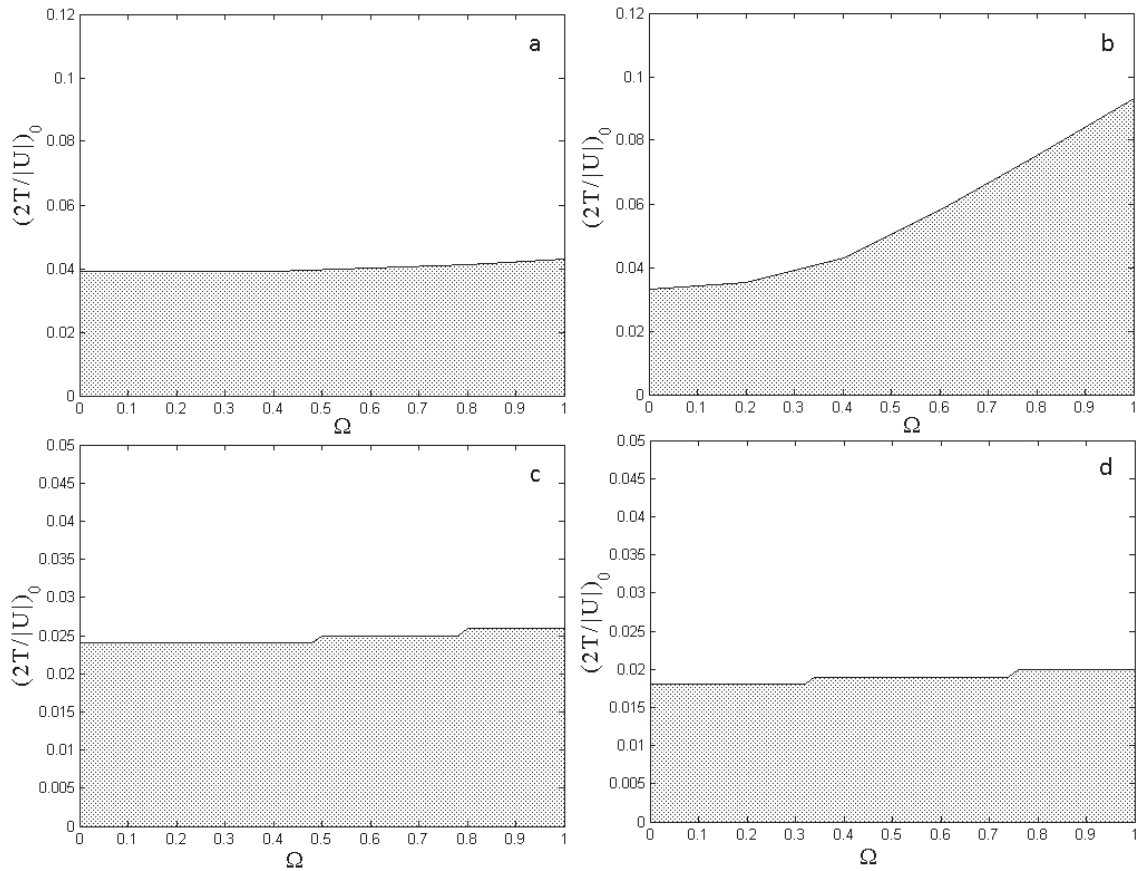


**Fig. 1.** Critical dependences of the initial virial ratio on the rotation parameter for  $N = 11$  and  $m = 3$  (a),  $N = 12$  and  $m = 4$  (b),  $N = 14$  and  $m = 4$  (c), and  $N = 16$  and  $m = 6$  (d)

where

$$S_{1N} = \int_{-\infty}^{\psi} W^{-1} E \frac{dP_N(\cosh)}{d \cosh} d\psi_1,$$

$$S_{2N} = \int_{-\infty}^{\psi} W^{-1} E \sinh \frac{d^2 P_N(\cosh)}{d(\cosh)^2} d\psi_1.$$

Here,

$$\cos h = \frac{c(\lambda + \cos \psi_1) + e^2 s \sin \psi_1}{(1 + \lambda \cos \psi)(1 + \lambda \cos \psi_1)},$$

$$E = \frac{1}{e^6} (1 + \lambda \cos \psi_1)^3 S(\psi, \psi_1) A(\psi_1),$$

$$W = \frac{1 + \lambda \cos \psi_1}{1 + \lambda \cos \psi}, \quad c = \lambda + \cos \psi, \quad s = \sin \psi.$$

(see the other notations in works [20–22, 25]).

#### 4. Analysis of Small-Scale Instabilities

We consider a model, in which the formation of an SGSC at the early stage of the protogalaxy collapse is associated with a gravitational instability of the nonlinear nonstationary model with respect to high-order vibrational modes. The latter correspond to rather small-scale perturbations of the density in the collapsing galaxy. The mode order determines the average number of GSCs in the system. According to the SGSC classification [5], a system is called poor, if the number of GSCs in it falls within the interval from 10 to 100, and moderate, if from 100 to 1000. Here, we will consider four modes of vibrations:  $(N = 11, m = 3)$ ,  $(N = 12, m = 4)$ ,  $(N = 14, m = 4)$ , and  $(N = 16, m = 6)$ . The first two correspond to poor systems, and the last two to moderate ones. For the indicated modes of vibrations, an instability under certain initial conditions can result in the for-

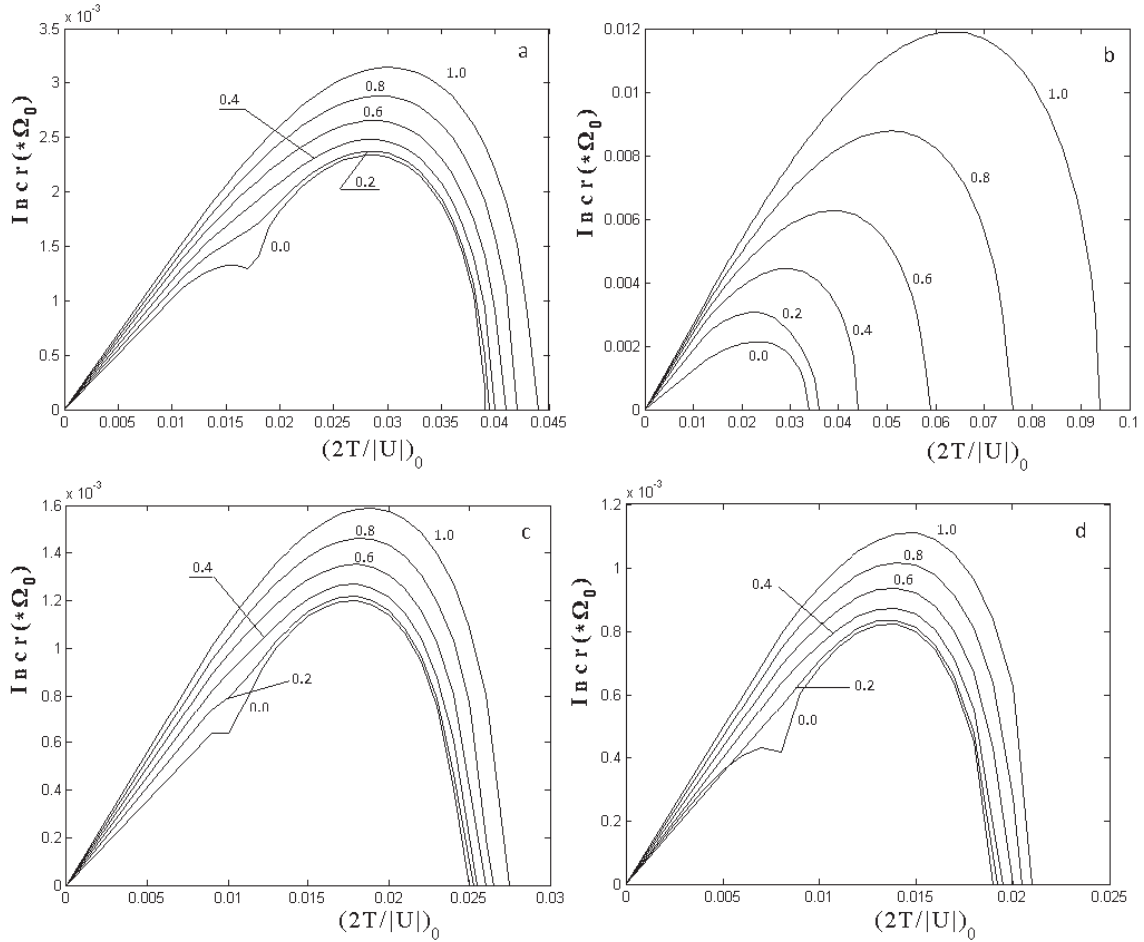


**Fig. 2.** Dependences of instability growth rates on the parameters  $(2T/|U|)_0$  and  $\Omega$  for  $N = 11$  and  $m = 3$  (a),  $N = 12$  and  $m = 4$  (b),  $N = 14$  and  $m = 4$  (c), and  $N = 16$  and  $m = 6$  (d). The corresponding values of the rotation parameter are indicated

mation of a system from clusters. The number of the latter will correspond to the case of poor or moderate SGSCs.

Note that the calculations of high-order modes give rise to cumbersome systems of integral or differential equations. For example, in the simple case ( $N = 11, m = 3$ ), we obtain a system of differential equations of the 44-th order:

$$(1 + \lambda \cos \psi) \frac{d^2 \gamma_\tau}{d\psi^2} + \lambda \sin \psi \frac{d\gamma_\tau}{d\psi} + \gamma_\tau = (1 + \lambda \cos \psi)^3 (\lambda + \cos \psi)^{N-\tau} \sin^{\tau-1} \psi A(\psi), \quad (8)$$

where

$$A(\psi) = \frac{1}{(1 + \lambda \cos \psi)^{20}} K_{11}^3(\gamma_\tau), \quad \tau = \overline{1, 11},$$

$$\gamma_\tau = \int_{-\infty}^{\psi} (1 + \lambda \cos \psi_1)^3 S(\psi, \psi_1) a(\psi_1) \times (\lambda + \cos \psi_1)^{N-\tau} \sin^{\tau-1} \psi_1 d\psi_1. \quad (9)$$

The expression for the function  $K_{11}^3$  is given in the Appendix.

In order to solve the NADE in the form of Eqs. (8) and (9), we have to change from the integral form to the differential one. By analogy with Eqs. (4) and (5), we use Eq. (9) to find a system of differential equations of the 44-th order,

$$(1 + \lambda \cos \psi) \frac{d^2 \gamma_\tau}{d\psi^2} + \lambda \sin \psi \frac{d\gamma_\tau}{d\psi} + \gamma_\tau = (1 + \lambda \cos \psi)^3 (\lambda + \cos \psi)^{N-\tau} \sin^{\tau-1} \psi A(\psi).$$

Hence, we obtained a system of differential equations of the 44-th order in the case ( $N = 11, m = 3$ ). The NADEs for other – (12,4), (14,4), and (16,6) – modes of vibrations are even more cumbersome and, therefore, are not presented here. In the mentioned cases, the corresponding systems have 80, 120, and 180 clusters, respectively. The corresponding vibrational modes are described by the systems of differential equations of the 48-th, 56-th, and 64-th orders, respectively.

### 5. Results and Their Discussion

The instabilities of four indicated vibrational modes were studied numerically by solving the corresponding NADE separately for each mode. Every time, the instability regions in the diagram “initial virial ratio versus rotation parameter of the model” had to be determined for the specific perturbation mode, by using the method of periodic solution stability [27]. We also found the corresponding dependences of the instability growth rate on the virial ratio value at the beginning of the collapse.

In Fig. 1, the critical dependences of the initial virial ratio on the rotation parameter are shown. One can see that, as the mode order grows, the critical value of the initial virial parameter decreases, so that the instability region slowly becomes narrower. In general, the instability rate depends very weakly on the rotation degree of a collapsing protogalaxy.

Figure 2 illustrates the behavior of instability growth rates and its dependence on the virial ratio and the rotation parameter. In each case, the values of instability growth rates increase with the rotation parameter. The calculations show that the corresponding instability region begins at small values of the virial parameter, e.g.,  $(2T/|U|)_0 = 0.024$  for the mode (14,4) and  $(2T/|U|)_0 = 0.018$  for the mode (16,6). The both indicated values of the virial ratio correspond to the rotation absence, and the rotation switching-on results in the destabilization.

We also compared the instability growth rates of four vibrational modes at fixed rotation parameter values. It should be noted that, among the examined vibrational modes, mode (12,4) remained to be a leader at every rotation parameter value. With the increase of the vibrational mode order, the instability growth rates gradually diminish.

Note that the analogy between a gas medium with an adiabatic index of  $5/3$  and a star system, which

was used in this work for real objects, gives approximate estimates for the physical state at the collapse beginning and the instability. For example, from the condition found for the virial ratio in the case of mode (14,4), we determined the critical temperature for a protogalaxy, which turned out to be equal to  $5.2 \times 10^4$  K. Our calculations show that the formation of the SGSC occurs due to the instability of radial motions in the protogalaxy.

*The work was carried out in the framework of the grant OT-F2-13 of the Science and Technology Agency of the Republic of Uzbekistan.*

### APPENDIX

$$\begin{aligned}
 K_{11}^3(\gamma_r) = & \left( 3c^{10} + \frac{945}{128}c^2e^8s^8 - \frac{63}{512}e^{10}s^{10} - \right. \\
 & \left. - \frac{1575}{32}c^4e^6s^6 - \frac{135}{4}c^8e^2s^2 + \frac{315}{4}c^6e^4s^4 \right) \gamma_1 + \\
 & + \left( \frac{4095}{256}e^{10}s^9c - \frac{4095}{16}e^8s^7c^3 + \frac{195}{2}c^9e^2s + \right. \\
 & \left. + \frac{12285}{16}c^5e^6s^5 - 585c^7e^4s^3 \right) \gamma_2 + \\
 & + \left( \frac{82215}{32}c^4e^8s^6 - \frac{135}{4}c^{10}e^2 - \frac{114345}{32}c^6e^6s^4 - \right. \\
 & \left. - \frac{214515}{512}e^{10}s^8c^2 + \frac{945}{128}e^{12}s^{10} + \frac{2295}{2}c^8e^4s^2 \right) \gamma_3 + \\
 & + \left( \frac{48555}{8}c^7e^6s^3 + \frac{241605}{64}c^3e^{10}s^7 - 585c^9e^4s - \right. \\
 & \left. - \frac{4095}{16}ce^{12}s^9 - \frac{159705}{16}e^8s^5c^5 \right) \gamma_4 + \\
 & + \left( -\frac{114345}{32}e^6s^2c^8 + \frac{1020915}{64}e^8c^6s^4 + \right. \\
 & \left. + \frac{82215}{32}e^{12}c^2s^8 + \frac{315}{4}e^4c^{10} - \right. \\
 & \left. - \frac{1575}{32}e^{14}s^{10} - \frac{3569895}{256}e^{10}c^4s^6 \right) \gamma_5 + \\
 & + \left( \frac{12285}{16}e^6sc^9 + \frac{2803437}{128}e^{10}c^5s^5 - \frac{159705}{16}e^8c^7s^3 + \right. \\
 & \left. + \frac{12285}{16}e^{14}s^9c - \frac{159705}{16}e^{12}s^7c^3 \right) \gamma_6 + \\
 & + \left( \frac{1020915}{64}e^{12}c^4s^6 - \frac{114345}{32}e^{14}s^8c^2 - \right. \\
 & \left. - \frac{1575}{32}e^6c^{10} - \frac{3569895}{256}e^{10}c^6s^4 + \right. \\
 & \left. + \frac{82215}{32}e^8s^4c^6 + \frac{82215}{32}e^8c^8s^2 \right) \gamma_7 + \\
 & + \left( -585e^{16}cs^9 - \frac{159705}{16}e^{12}c^5s^5 + \frac{48555}{8}e^{14}c^3s^7 - \right. \\
 & \left. - \frac{4095}{16}e^8sc^9 + \frac{241605}{64}e^{10}c^7s^3 \right) \gamma_8 +
 \end{aligned}$$

$$\begin{aligned}
 & + \left( \frac{2295}{2} e^{16} c^2 s^8 + \frac{945}{128} e^8 c^{10} - \right. \\
 & - \frac{135}{4} e^{18} s^{10} - \frac{114345}{32} e^{14} s^6 c^4 - \\
 & \left. - \frac{214515}{512} e^{10} c^8 s^2 + \frac{82215}{32} e^{12} c^6 s^4 \right) \gamma_9 + \\
 & + \left( \frac{4095}{256} e^{10} c^9 s - \frac{4095}{16} e^{12} s^3 c^7 + \frac{195}{2} e^{18} s^9 c - \right. \\
 & - 585 e^{16} s^7 c^3 + \frac{12285}{16} e^{14} c^5 s^5 \left. \right) \gamma_{10} + \\
 & + \left( 3e^{20} s^{10} + \frac{945}{128} e^{12} c^8 s^2 - \frac{135}{4} e^{18} c^2 s^8 - \right. \\
 & - \frac{1575}{32} e^{14} c^6 s^4 + \frac{315}{4} e^{16} s^6 c^4 - \frac{63}{512} e^{10} c^{10} \left. \right) \gamma_{11} + \\
 & + im\Omega \left\{ \left( -\frac{189}{32} s^5 e^5 c^5 + \frac{9}{2} s^3 c^7 e^3 - \right. \right. \\
 & - \frac{63}{512} s^9 c e^9 + \frac{63}{32} s^7 c^3 e^7 - \frac{3}{4} e s c^9 \left. \right) \gamma_1 + \\
 & + \left( \frac{3591}{512} c^2 e^9 s^8 - \frac{63}{512} s^{10} e^{11} + \frac{1953}{32} c^6 e^5 s^4 - \right. \\
 & - \frac{693}{16} c^4 e^7 s^6 + \frac{3}{4} c^{10} e - \frac{81}{4} c^8 e^3 s^2 \left. \right) \gamma_2 + \\
 & + \left( -\frac{13419}{128} c^3 e^9 s^7 + \frac{567}{2} c^5 e^7 s^5 - \frac{2889}{16} c^7 e^5 s^3 + \right. \\
 & + \frac{81}{4} c^9 e^3 s + \frac{3591}{512} c e^{11} s^9 \left. \right) \gamma_3 + \\
 & + \left( \frac{63}{32} s^{10} e^{13} + \frac{75159}{128} c^4 e^9 s^6 - \frac{13419}{128} c^2 e^{11} s^8 - \right. \\
 & - \frac{9}{2} c^{10} e^3 - \frac{22743}{32} c^6 e^7 s^4 + \frac{2889}{16} c^8 e^5 s^2 \left. \right) \gamma_4 + \\
 & + \left( \frac{75159}{128} c^3 e^{11} s^7 - \frac{353241}{256} c^5 e^9 s^5 + \right. \\
 & + \frac{22743}{32} c^7 e^7 s^3 - \frac{693}{16} c e^{13} s^9 - \frac{1953}{32} c^9 e^5 s \left. \right) \gamma_5 + \\
 & + \left( \frac{567}{2} c^2 e^{13} s^8 + \frac{353241}{256} c^6 e^9 s^4 - \frac{353241}{256} c^4 e^{11} s^6 + \right. \\
 & + \frac{189}{32} c^{10} e^5 - \frac{567}{2} c^8 e^7 s^2 - \frac{189}{32} e^{15} s^{10} \left. \right) \gamma_6 + \\
 & + \left( \frac{353241}{256} c^5 e^{11} s^5 + \frac{693}{16} c^9 e^7 s - \frac{75159}{128} c^7 e^9 s^3 - \right. \\
 & - \frac{22743}{32} c^3 e^{13} s^7 + \frac{1953}{32} c e^{15} s^9 \left. \right) \gamma_7 + \\
 & + \left( \frac{9}{2} e^{17} s^{10} + \frac{22743}{32} c^4 e^{13} s^6 - \frac{75159}{128} c^6 e^{11} s^4 - \right. \\
 & - \frac{63}{32} c^{10} e^7 + \frac{13419}{128} c^8 e^9 s^2 - \frac{2889}{16} c^2 e^{15} s^8 \left. \right) \gamma_8 + \\
 & + \left( -\frac{567}{2} c^5 e^{13} s^5 + \frac{2889}{16} c^3 e^{15} s^7 - \frac{3591}{512} c^9 e^9 s - \right. \\
 & - \frac{81}{4} c e^{17} s^9 + \frac{13419}{128} c^7 e^{11} s^3 \left. \right) \gamma_9 + \\
 & + \left( -\frac{1953}{32} c^4 e^{15} s^6 + \frac{693}{16} c^6 e^{13} s^4 - \frac{3}{4} e^{19} s^{10} + \right.
 \end{aligned}$$

$$\begin{aligned}
 & + \frac{63}{512} c^{10} e^9 - \frac{3591}{512} c^8 e^{11} s^2 + \frac{81}{4} c^2 e^{17} s^8 \left. \right) \gamma_{10} + \\
 & + \left( \frac{63}{512} c^9 e^{11} s + \frac{189}{32} c^5 e^{15} s^5 - \frac{9}{2} c^3 e^{17} s^7 - \right. \\
 & \left. - \frac{63}{32} c^7 e^{13} s^3 + \frac{3}{4} c e^{19} s^9 \right) \gamma_{11} \left. \right\}.
 \end{aligned}$$

1. K. Ashman, S. Zepf. *Globular Cluster Systems* (Cambridge Univ. Press, 1998).
2. K. Gebhardt, M. Kissler-Pating. Globular cluster systems. I. V-I color distributions. *Astron. J.* **118**, 1526 (1999).
3. W.E. Harris, G.L. Harris, A. Matthew. A catalog of globular cluster systems: What determines the size of a galaxy's globular cluster population? *Astrophys. J.* **772**, 82 (2013).
4. W.E. Harris, W. Morningstar *et al.* Globular cluster systems in brightest cluster galaxies: A near-universal luminosity function? *Astrophys. J.* **797**, 128 (2014).
5. S.N. Nuritdinov, I.U. Tadjibaev. Globular star cluster systems around galaxies. I. Search for statistical relationships. *Astrophys.* **57**, 59 (2014) (in Russian).
6. I.U. Tadjibaev, S.N. Nuritdinov, J.M. Ganiev. Globular star cluster systems around galaxies. II. Spiral and dwarf galaxies. *Astrophys.* **58**, 181 (2015) (in Russian).
7. W.E. Harris. Where are most of the globular clusters in today's universe? *Astron. J.* **151**, 102 (2016).
8. Ya.B. Zel'dovich, I.D. Novikov. *The Structure and Evolution of the Universe* (Univ. of Chicago Press, 1983).
9. P.J.E. Peebles, R.H. Dicke. Origin of the globular star clusters. *Astrophys. J.* **154**, 891 (1968).
10. K.M. Ashman, S.E. Zepf. The formation of globular clusters in merging and interacting galaxies. *Astrophys. J.* **384**, 50 (1992).
11. S.M. Fall, M.J. Rees. A theory for origin of globular clusters. *Astrophys. J.* **298**, 18 (1985).
12. A. Forbes, J.P. Brodie, C.J. Grillmair. On the origin of globular cluster systems in elliptical and cD galaxies. *Astron. J.* **113**, 1652 (1997).
13. Ch. Theis. How to form (twin) globular clusters? *ASP Conf. Ser.* **228**, 347 (2001).
14. W.E. Harris. Globular clusters and galaxy mergers. *Astrophys. J.* **251**, 497 (1981).
15. F. Schweizer. Star formation in colliding and merging galaxies. In: *Nearly Normal Galaxies*, edited by S.M. Faber (Springer, 1987), p. 18–25.
16. F. Schweizer. The nature of elliptical galaxies. *ASP Conf. Ser.* **116**, 447 (1997).
17. J.P. Brodie, L.L. Schrodes *et al.* Keck spectroscopy of candidate 97 proto-globular clusters in NGC 1275. *Astron. J.* **116**, 691 (1998).
18. S.N. Nuritdinov, Zh.R. Orazimbetov, I.U. Tadjibaev. To the problem of formation of globular clusters system. In: *Variable Stars: A Key to Understand the Galaxy Structure and Evolution* (Nijniy Arxyz, 2000), p. 197 (in Russian).

19. J. Binney, S. Tremaine. *Galactic Dynamics* (Princeton Univ. Press, 2008).
20. V.A. Antonov, S.N. Nuritdinov. Instability of a nonlinearly pulsating model stellar system. I – an Einstein sphere. *Astron. Zh.* **58**, 1158 (1981) (in Russian).
21. S.N. Nuritdinov. Instability of a nonlinearly pulsating model stellar system. II. *Astron. Zh.* **60**, 40 (1983) (in Russian).
22. S.N. Nuritdinov. *Early Evolution of Galaxies: Nonlinear Models and Instabilities* (Tashkent Univ., 2003) (in Russian).
23. C.L. Camm. Self-gravitating star systems. II. *Mon. Not. R. Astron. Soc.* **112**, 115 (1952).
24. S.N. Nuritdinov. Instability of a nonlinearly pulsating model of a stellar system – Volume perturbations: Camm's model. *Astron. Zh.* **68** (4), 763 (1991) (in Russian).
25. S.N. Nuritdinov. A new series of non-stationary models of the galactic subsystems: The rotation case. *Astron. Tsirk. BAS AN* **1553**, 9 (1992) (in Russian).
26. V.L. Polyachenko, A.M. Fridman. *Equilibrium and Stability of Gravitating Systems* (Nauka, 1976) (in Russian).

27. I.G. Malkin. *Theory of Stability of Motion* (Nauka, 1966).

Received 25.08.17.

Translated from Ukrainian by O.I. Voitenko

I.U. Таджібаєв, С.Н. Нурітдінов, А.А. Мумінов

## НЕЛІНІЙНА КОСМОЛОГІЯ СИСТЕМИ КУЛЬОВИХ СКУПЧЕНЬ НАВКОЛО ГАЛАКТИК

### Резюме

Вивчено питання походження систем кульових скупчень зірок навколо галактик на тлі нелінійно нестационарної моделі колапсуєчих галактик. Досліджено нестійкості даної нелінійної моделі щодо чотирьох дрібномасштабних мод збурень. При цьому ступінь моди визначає в середньому кількість скупчень в системі. Побудовано критичні діаграми залежності початкового значення віриалів відношення від ступеня обертання колапсуєчої моделі. Обчислені значення інкрементів відповідних видів нестійкостей. Виконано порівняння результатів розрахунку характеристик нестійкостей розглянутих мод коливань.